Nat. Hazards Earth Syst. Sci. Discuss., 2, 4421–4438, 2014
www.nat-hazards-earth-syst-sci-discuss.net/2/4421/2014/
doi:10.5194/nhessd-2-4421-2014

Natural Hazards and Earth System Sciences
Open Access
Discussions

Study of the seismicity temporal variation for the current seismic hazard evaluation in Val d'Agri, Italy

I. Baskoutas[1], **G. A. Papadopoulos**[2], **and A. D'Alessandro**[3]

[1]Institute of Geodynamics, National Observatory of Athens, Athens, Greece
[2]Earthquake Planning and Protection Organization, Seismotect. Div., Xanthou 32, 15451 Athens, Greece
[3]Istituto Nazionale di Geofisica e Vulcanologia, Centro, Nazionale Terremoti, Rome, Italy

Received: 22 April 2014 – Accepted: 5 May 2014 – Published: 19 June 2014

Correspondence to: I. Baskoutas (i.basko@noa.gr),
G. Papadopoulos (gpapadopoulos@oasp.gr),
and A. D'Allesandro (antonino.dalessandro@ingv.it)

Published by Copernicus Publications on behalf of the European Geosciences Union.

Abstract

This study examines the temporal variation of the seismicity in the Val d'Agri (Southern Italy) and adjacent areas, for the current seismic hazard evaluation. The temporal variation of the seismicity is expressed as time series of the number of earthquakes, the b value of the frequency magnitude distribution of Gutenberg-Richter relationship and the seismic energy released in the form of $\log E^{2/3}$. The analysis was performed by the means of a new research tool that includes visualizing techniques, which helps the interactive exploration and the interpretation of temporal variation changes. The obtained time series show a precursory seismicity pattern, characterized by low and high, probability periods, which preceded earthquakes of magnitude $M \geq 4.0$. 75 % of the examined cases were successfully correlated and 25 of them resulted false. The average duration of the low and the high probability periods is 10.6 and 13.8 months long respectively. These results indicate that the seismicity temporal variation monitoring in given area and the recognition of the low and high probability periods, can contribute to the evaluation, in regular monthly intervals, of the current status seismic hazard.

1 Introduction

Val d'Agri is the most seismically active sector of the central-western Mediterranean region, having repeatedly struck by destructive earthquakes in 1561 ($M = 6.5$), 1857 ($M = 7$) and 1980 ($M = 6.9$). Earthquakes are characterized by predominant normal-faulting focal mechanisms, with NW-oriented nodal planes, occur within a narrow seismic belt, about 20 to 40 km wide, centered on the axis of the Apennine chain (Amato et al., 1997; Selvaggi, 1998; Valensise and Pantosti, 2001). Seismicity occurs mainly along the major seismogenic structures, such as the Irpinia Fault, which slipped during the 1980 M 6.9 normal-faulting event, but also at the boundary between adjacent fault segments of the active belt.

NHESSD
2, 4421–4438, 2014

The Val d'Agri instrumental seismicity recorded in the last 30 years is low and sparse showing only two small seismic swarms recorded between April–June 1996 and February–December 2002. The first swarm was characterized by low-magnitude events (M_d = 1.8–3.4), to the south of the basin at 2–7 km depth (Cucci et al., 2004). The second swarm consists of very few earthquakes with magnitudes ranging between 2.2 and 3.2, also clustering to the south of the Agri basin (Frepoli et al. 2005).

In this area there are many environmental protected zones and natural parks, a sequence of shallow and deep aquifers and hydraulic network systems for storage and supply water for agricultural and civil purposes, therefore the seismic hazard evaluation is a very important task. Usually to asses the seismic hazard, the most widespread and internationally accepted method is to estimating the peak ground strong motion expected in a given place by applying probabilistic or deterministic methodologies. Nevertheless the evaluation of the seismic hazard and especially its current status, by monitoring its level, is also another promising task for area of such multifunctional activities.

This study examines the temporal variation of the seismicity in the Agri valley (Southern Italy) and adjoining region in the period 1983–2013 for the current status of the seismic hazard evaluation by means of FastBEE tool (Papadopoulos and Baskoutas, 2009, 2011). This tool is suited to visualize simultaneously the temporal variation curves of common seismicity parameters like, the number of earthquakes N that occurs in a certain magnitude range, the *b* value of the frequency magnitudes distribution relation and the seismic energy released, supposing that they depict the influence of the tectonic stress and to explore their temporal behavior in terms of probability periods for an earthquake occurrence. In fact, among these parameters, it is well established that *b* value is related to the seismogenic procedure containing information on differences in the physics of the process that generates earthquakes (Aki, 1965; Smith, 1986; Imoto 1991; Monterroso, 2003) and that depends on the stress condition and on the homogeneity of the material in the focal region being useful for seismicity interpretation (Mogi, 1967; Scholz, 1968; Wyss, 1973; Wiemer, 2002). On the other hand, the seismic energy released reveals the build-up and release of stress, depending of geotectonic characteristics. Keilis-Borok (1959) and Sadovski and Pisarenko (1983) have proposed that seismic energy in the form $\log E^{2/3}$, being from the physical point of view proportional to the rate of accumulation of the dynamic ruptures in the strong earthquakes preparation process area, may reflect the variations of the tectonic stress in the region of the observation.

2 Method

FastBEE algorithm, based on the character of the seismicity parameters described previously described, assumes that the temporal variation curves of these parameters represent distinct phases of a phenomenological model for the strong earthquakes preparation (Popandopoulos and Baskoutas, 2011) and can be explained according to the classical models for the preparation of earthquakes and especially the phases of the consolidation model (Dobrovolski, 1991).

The characteristic onset of the temporal change, where the amount of the released seismic energy $\log E^{2/3}$, decreases and the simultaneous b value increases as well the consequent changes of both parameters i.e. increases of the seismic energy released and decreases of b value, is characterized by two distinct and consecutive low and high probability stages before a strong earthquake occurrence (Fig. 1). This behavior was formulated as precursory seismicity pattern (Baskoutas et al., 2011; Baskoutas and Popandopoulos, 2014).

Based on the above consideration, the methodology for the current seismic hazard evaluation consists:

First in the construction, by the means of FastBEE tool, of the temporal variation series of a set of seismicity parameters, like the number of earthquakes N, b value and the seismic energy released in the form $\log E^{2/3}$.

Second in the correlation of the observed temporal variation series changes with the significant for the area earthquakes.

The magnitude of these events represent the lower magnitude that correlates better the observed temporal changes and was determined, by retrospective analysis of all available seismic data in the examined area. According to the FastBEE algorithm, these events depend on the seismotectonic characteristics of the area and represent, from the physical point of view, a representative response of the medium to the topic tectonic stress acting in the area

The number of earthquakes per unit time, $\log N$, is obtained by the means of the follow formula:

$$\log N(t) = \log \left(\sum_{i=t-w}^{n(t-w)} i \right) \tag{1}$$

where i is the number of earthquakes, with magnitude $M_w > M_{min}$, M_{min} is the minimum magnitude of the catalogue completeness, in a given area and time interval, t is the time interval of one month, w is the length of the smoothing (filter) window, $n(t-w)$ is the number of earthquakes in the smoothing window time interval. The standard error of the calculation is given by the relation: $\sigma_{\lg N} = 0.4343/\sqrt{N}$

Estimates of b value are obtained using the maximum likelihood estimation method by the means of the relationship proposed by Gusev (1974) as follow:

$$b(t) = \log \left[1 + \frac{N_\Sigma(t-w)}{\sum_{i=0}^{n} i \cdot N_{M_{min}} + i\,\Delta M(t-w)} \right] / \Delta M \tag{2}$$

where N_Σ is the total number of earthquakes, with magnitude $M_w > M_{min}$, M_{min} is the minimum completeness magnitude, in a given area and time interval, $N_{M_{min}} + i\,\Delta M$

NHESSD
2, 4421–4438, 2014

Title Page
Abstract | Introduction
Conclusions | References
Tables | Figures
◀| |▶
◀ ▶
Back | Close
Full Screen / Esc
Printer-friendly Version
Interactive Discussion

is the number of earthquakes in the ith magnitude, $n = 1 + (M_{\max} - M_{\min})/\Delta M$ is the number of the increment $\Delta M = 0.20$. The standard error of the b value estimates is obtained by means of the relation: $\sigma_b(t) = b(t)/\sqrt{N_\Sigma}$.

Finally $\log E^{2/3}$, which expresses the mean seismic energy released per unit time, is obtained using the follow relation:

$$\log E^{2/3}(t) = \log\left(\frac{1}{n(t-w)}\sum_{i=t-w}^{n(t-w)} e_i^{2/3}\right) \tag{3}$$

where t is the time interval in months, $n(t-w)$ is the number of earthquakes in the smoothing window time interval. E_i is the seismic energy of the ith earthquake in the time window w. The confidence limits were calculated in the range of the examined time period and they were considered as a measure of the statistical significance.

3 Data and analysis

This analysis use seismic data, in the period 1983–2014, from an area bounded by the coordinates 39°70′–41°10′ N and 15°10′–16°50′ E, which includes the two main sources in the neighborhood of Seismotectonic Val d'Agri region. The data, which were taken from the earthquakes catalogue of the National Institute of Geophysics and Volcanology (INGV) of Rome (Fig. 2) are complete for events with magnitudes $M \geq 2.5$ for the entire examine period. Their completeness was examined by means of the discrete frequency magnitude distribution (Fig. 3).

Figure 3 show, from the top to at the bottom, the temporal variation of the seismic parameters $\log N$, b value and $\log E^{2/3}$ and their rms scatter (1σ) of the data, corresponding to a 70 % confidence interval. These errors are reported in this graph as horizontal lines, on either side of the average value in the case of the parameters $\log N$ and $\log E^{2/3}$. The standard error of the b value estimate refers at each step of averaging. The temporal variation curves of the examined parameters were obtained using a moving window almost 1 year long and with step of one month.

The numbered arrows, perpendicular to the time axis show the origin times of all events with $M \geq 4.0$ (Table 1), which epicenter can be seen as solid stars in Fig. 2. These events determined in an error and trial iterative procedure, as was pointed out earlier, report the lower magnitude earthquakes threshold that occurred in the area and fit better with the observed significant temporal variation changes. Because of the low seismicity, the number of earthquakes as the variance of magnitudes, which in many cases is less than 2.5, do not allow reliable calculation of *b* value, (as illustrated in Fig. 3) and hence will not be taken into account in the analysis. Therefore the analysis will be based on the identification of the discrete, low and high probability periods of the precursory seismicity pattern (Fig. 1) on parameter $\log E^{2/3}$ time series only (Fig. 5).

The inspection of Fig. 5 shows the existence of consecutive relative minima and maxima, over and above the mean value of the examined parameters. In the same figure, can be seen also that the earthquakes with magnitude $M \geq 4.0$ (Table 1) are correlated with distinct phases of the above mentioned precursory seismicity pattern. Namely, both parameters show initially a decreasing stage starting from a preceding relative maximum advancing toward to a relative minimum. It is observed that this time period practically is characterized by the absence of significant earthquakes and for this reason constitute the low probability stage (solid rectangles in Fig. 5). The change of this trend coincides with the appearance of the relative, $\log E^{2/3}$ and $\log N$ minima after that shows an increasing period.

It is clear that, almost all earthquakes occur during this period showing thus that this period can be considered as highly probability period for the occurrence of an earthquake $M \geq 4.0$. Practically the appearance of the relative minimum, in the majority of the examined cases, signalizes the beginning of the alarm period lasting until the earthquake occur, unless this behaviour changes. Earthquakes 1 and 2 of Table 1 can not be analysed, because there are not data before 1983.

4 Results

The identification of the relative maxima and minima that represent the beginning of the two probability periods can be measured directly on these graphs or by analyzing the appropriate temporal variation series.

Table 2 report the dates of the appearance of the relative maximum, that practically signalizes the beginning of the low probability period and relative minimum which signalizes the high and their respective duration, in months, which were measured using the temporal variation estimates of the parameter $\log E^{2/3}$.

Both qualitative and quantitative analysis shows that six (6) of the eight (8) cases, i.e. 75 %, of the relative minima that appears on $\log E^{2/3}$ curve, were followed by one or by a group of earthquakes, with magnitude $M \geq 4.0$. Instead there are two relative minimum, i.e. 25 % of the cases, which were not followed by earthquake, therefore these cases can be considered as false alarms. The first of them started at November 1993 and ended at October 1994 and the second started at July 2000 and ended at October 2001.

Is interesting to point out that the temporal variation analysis of the seismic parameters reveal a period of stable seismic activity, which was started at the beginning of the year 2006 and ended in the year 2009.

5 Conclusions

The seismicity temporal variation analysis shows significant temporal changes, in all three examined seismicity parameters, using data from the Val d'Agri region in the periods 1983–2013.

The form of these changes, that fluctuates around parameters mean values in the examined over a 30-year period of observations, shows clear regularity corresponding to phases of a phenomenogical model of earthquake preparation process. Therefore,

NHESSD
2, 4421–4438, 2014

these changes were supposed that depict the response of the medium in the examined period due to the stress acting in the wider area.

Six of the eight cases of earthquakes with magnitude $M \geq 4.0$, which occurred in this area, were successful correlated with the precursory seismicity pattern, low and high probability periods. The mean duration of the low probability period, for an earthquake occurrence with magnitude $M \geq 4.0$ is about 10.6 months, while the respective high probability period is 13.8 months.

In accordance with the above findings, the evaluation of the temporal variation of seismic parameters until the 2013 shows that the region is going through a period of low probability for an earthquake occurrence with a magnitude above $M \geq 4.0$, unless the temporal behaviour changes. These results indicate that the continuous monitoring of the seismicity temporal variation, by means of FastBEE tool, permits the evaluation of the current seismic hazard in regular intervals, in given area.

References

Aki, K.: Maximum likelihood estimate of b in the formula $\log N = a - bM$ and its confidence limits, Bull. Earthq. Res. Inst. Univ. Tokyo, 43, 237–239, 1965.

Amato, A., Chiarabba, C., and Selvaggi, G.: Crustal and deep seismicity in Italy (30 years after), Ann. Geofis., 40–5, 981–994, 1997.

Baskoutas, I. and Popandopoulos, G.: Qualitative precursory pattern before several strong earthquakes in Greece, Res. Geophys., 4, 4899, doi:10.4081/rg.2014.4899, 2014.

Baskoutas, I., Papadopoulos, G., and Chingtham, Pr.: Temporal variation of seismic parameters in the western part of the India-Eurasia Plate Collision Zone, Res. Geophys., doi:10.4081/rg.2011.e3, online first, 2011.

Cucci, L., Pondrelli, S., Frepoli, A., Mariucci, M. T., and Moro, M.: Local pattern of stress field and seismogenic sources in Melandro Pergola basin and in Agri valley (Southern Italy), Geophys. J. Int., 156, 575–583, 2004.

Dobrovol'skii, I. P.: Theory of Preparation of a Tectonic Earthquake, Inst. of the Phys. of the Earth. RAS, Publications, Moscow, 1991.

Frepoli, A., Cinti, F. R., Amicucci, L., Cimini, G. B., De Gori, P., and Pierdominici, S.: Pattern of seismicity in the lucanian Apennines (Southern Italy) from recording by SAPTEX temporary array, Ann. Geophys., 48, 1035–1054, 2005, http://www.ann-geophys.net/48/1035/2005/.

Gusev, A. A.: Earthquake prediction from statistical seismicity data, in Seismicity and Seismic Prediction, Upper Mantle Properties and Their Relation to the Kamchatka Volcanism, Nauka, Novosibirsk, 109–119, 1974.

Imoto, M.: Changes in the magnitude-frequency 6-value prior to large ($M = 6.0$) earthquakes in Japan, Tectonophysics, 193. 311–325, 1991.

Keilis-Borok, V. I.: On the estimation of the displacement in an earthquake source and of source dimensions, Annali di Geofisica 12, 205–214, 1959.

Mogi, K.: Earthquakes and fractures, Tectonophysics, 5, 35–55, doi:10.1016/0040-1951(67)90043-1, 1967.

Monterroso Juarez, D. A.: Statistical Seismology Studies in Central America, *b*-value, seismic hazard and seismic quiescence, Comprehensive Summaries of Uppsala Dissertations from the Faculty of Science and Technology, Acta Universitatis Upsaliensis, Uppsala, 897, 27, 2003.

Papadopoulos, G. A. and Baskoutas, I.: New tool for the spatio-temporal variation analysis of seismic parameters, Nat. Hazards Earth Syst. Sci., 9, 859–864, doi:10.5194/nhess-9-859-2009, 2009.

Popandopoulos, G. A. and Baskoutas, I.: Regularities in the Time Variations of the Seismic Parameters and Their Implications for Prediction of Strong Earthquakes in Greece, available online at: http://www.maik.ru/contents/physeth/physeth1011v47cont.htm, Izv Akad Nauk. Fiz Zemli, 11, 1–12, 2011.

Sadovski, M. A. and Pisarenko, V. F.: On the Dependence of the Duration of Earthquake Preparation on its Energy, Dokl. Akad. Nauk SSSR, 272, 330–333, 1983.

Scholz, C. H.: The frequency–magnitude relation of raicrofracturi'ng in rock and its relation to earthquakes, B. Seismol. Soc. Am., 58, 399–415, 1968.

Selvaggi, G.: Spatial distribution of horizontal seismic strain in the Apennines from historical earthquakes, Ann. Geofis., 41, 241–251, 1998.

Smith, W. D.: Evidence for precursory changes in the frequency magnitude *b*-value, Geophys. J. Roy. Astr. Soc., 86, 815–838, 1986.

NHESSD

2, 4421–4438, 2014

Seismicity temporal variation for the current seismic hazard evaluation in Val d'Agri

I. Baskoutas et al.

Valensise, G. and Pantosti, D.: The investigation of potential earthquake sources in peninsular Italy: a review, J. Seismol., 5, 287–306, 2001.
Wiemer, S. and Wyss, M.:. Spatial and temporal variability of the *b*-value in seismogenic volumes: An overview, Adv. Geophys., 45, 259–302, 2002.
Wyss, M.: Towards a physical understanding of the earthquake frequency distribution, R. Astron. Soc., 31, 341–359, 1973.

NHESSD
2, 4421–4438, 2014

Seismicity temporal variation for the current seismic hazard evaluation in Val d'Agri

I. Baskoutas et al.

Table 1. Strong earthquakes, $M_w \geq 5.6$, in the time period 1983–2013.

a/a	dd/mm/yy	Or. time	Lat	Lon	h	*M*
1	23 Jul 1986	08:19	40.64	15.77	6	4.2
2	5 May 1990	07:21	40.68	15.85	10	5.0
3	5 May 1990	07:38	40.68	15.79	5	4.4
4	28 Aug 1990	19:02	40.70	15.87	10	4.1
5	26 May 1991	12:26	40.61	15.70	5	4.5
6	29 May 1995	20:44	40.23	16.10	5	4.0
7	3 Apr 1996	13:04	40.68	15.53	5	4.5
8	9 Sep 1998	11:27	40.01	15.95	9	5.0
9	3 Sep 2004	00:04	40.70	15.68	5	4.0
10	28 May 2012	01:06	39.85	16.12	3	4.3
11	25 Oct 2012	23:05	39.88	16.01	6	5.0

NHESSD

2, 4421–4438, 2014

Seismicity temporal variation for the current seismic hazard evaluation in Val d'Agri

I. Baskoutas et al.

Table 2. Dates of the appearance of the relative maximum and minimum of the log $E2/3$ time series and the low and high probability periods duration.

a/a (group of Eqs.)	Date of max. appearance	Date of min. appearance	Low probability period duration	High probability period duration	Score
1	Dec 1984	May 1985	5	14	Success
2	May 1987	Sep 1988	15	20	Success
3	Dec 1990	Nov 1993	30	10	False (till Sep 1994)
4	Oct 1994	Feb 1995	4	3	Success
5	Sep 1996	Jan 1998	15	8	Success
6	Feb 1999	Jul 2000	16	14	False (till Oct 2001)
7	Oct 2001	Nov 2002	12	22	Success
8	Jan 2006–Dec 2007		46	Stable seismicity	
9	Nov 2010	Jan 2011	13	16	Success

NHESSD
2, 4421–4438, 2014

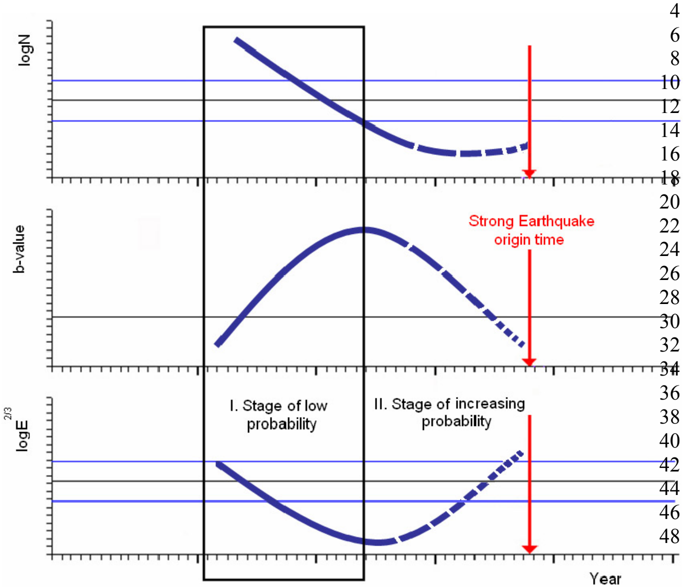

Figure 1. Characteristic FastBEE output schematic general trend of the temporal prognostic anomaly (solid blue lines) before a strong earthquake occurrence. The open rectangular parallelogram denotes the first, low probability stage, since the prognostic anomaly beginning, followed by a second higher probability stage, which conclude with the strong earthquake occurrence. Vertical red arrow shows the earthquake origin time (from Baskoutas and Popandopoulos, 2014).

NHESSD
2, 4421–4438, 2014

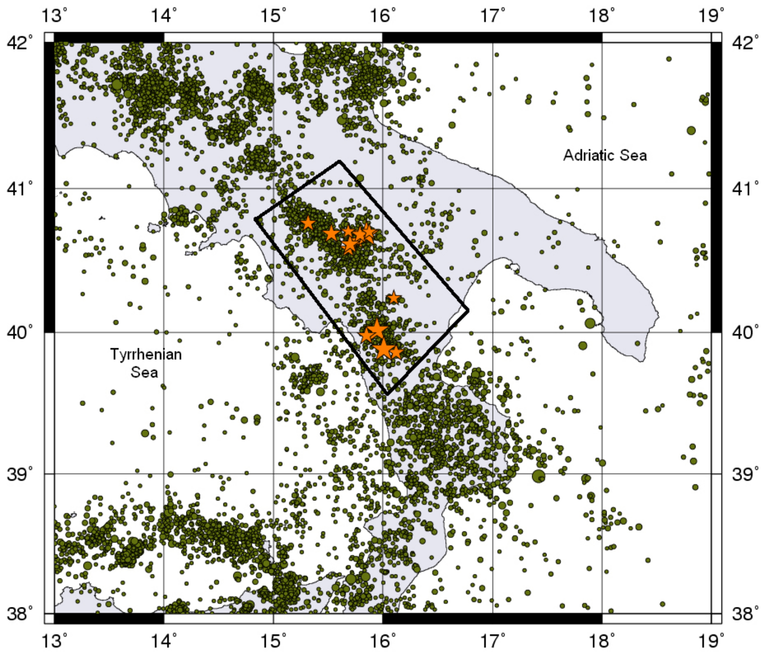

Figure 2. Seismicity map in the wider are of Val d'Agri region in the period 1983–2013 (open rectangle), used in the analysis. Solid stars show the strong earthquakes ($M \geq 4.0$) epicenters.

NHESSD
2, 4421–4438, 2014

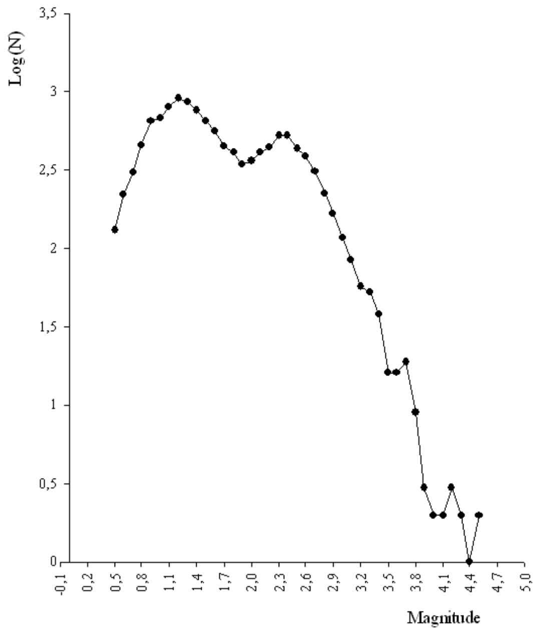

Figure 3. Non cumulative frequency magnitude distribution, in the period 1983–2013, denoting the changes of catalogue completeness.

NHESSD
2, 4421–4438, 2014

Seismicity temporal variation for the current seismic hazard evaluation in Val d'Agri

I. Baskoutas et al.

Title Page
Abstract | Introduction
Conclusions | References
Tables | Figures
◂ | ▸
Back | Close
Full Screen / Esc
Printer-friendly Version
Interactive Discussion

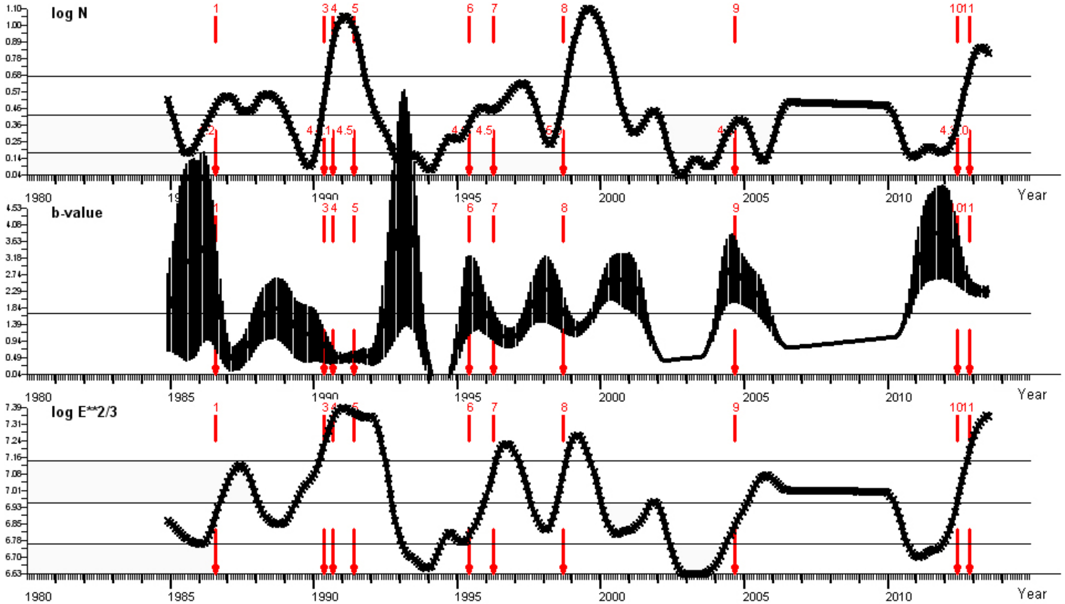

Figure 4. Temporal variation of the seismic parameters $\log N(t)$, b value and $\log E^{2/3}$, with their respective standard errors. Origin time and magnitude of all strong earthquakes, with magnitude $M \geq 4.0$ are shown as numbered arrows perpendicular to the time axis in the period 1983–2013.

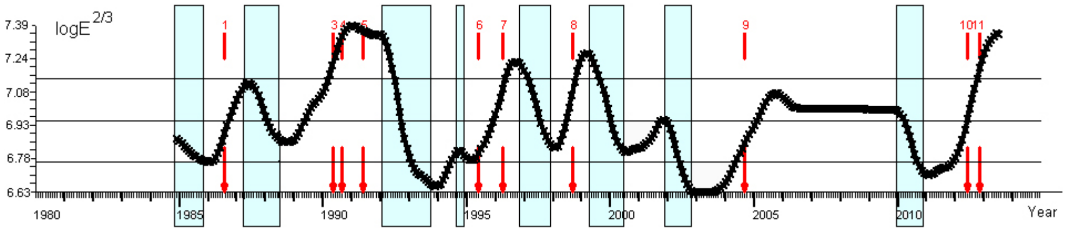

Figure 5. Temporal variation of log $E^{2/3}$. Numbered arrows perpendicular to the time axis denotes the origin time of all strong earthquakes, with magnitude $M \geq 4.0$. Solid rectangle shows the low probability periods for an earthquake occurrence which is followed by the consecutive high probability periods.

NHESSD
2, 4421–4438, 2014

Seismicity temporal variation for the current seismic hazard evaluation in Val d'Agri

I. Baskoutas et al.

Title Page
Abstract Introduction
Conclusions References
Tables Figures
◀ ▶
Back Close
Full Screen / Esc
Printer-friendly Version
Interactive Discussion